# Detection of breast abnormalities using a prototype resonance electrical impedance spectroscopy system: A preliminary study

Bin Zheng,[a] Margarita L. Zuley, Jules H. Sumkin, Victor J. Catullo, Gordon S. Abrams, Grace Y. Rathfon, Denise M. Chough, Michelle Z. Gruss, and David Gur
*Department of Radiology, University of Pittsburgh, Pittsburgh, Pennsylvania 15213*

(Received 6 February 2008; revised 23 April 2008; accepted for publication 24 April 2008; published 12 June 2008)

Electrical impedance spectroscopy has been investigated with but limited success as an adjunct procedure to mammography and as a possible pre-screening tool to stratify risk for having or developing breast cancer in younger women. In this study, the authors explored a new resonance frequency based [resonance electrical impedance spectroscopy (REIS)] approach to identify breasts that may have highly suspicious abnormalities that had been recommended for biopsies. The authors assembled a prototype REIS system generating multifrequency electrical sweeps ranging from 100 to 4100 kHz every 12 s. Using only two probes, one in contact with the nipple and the other with the outer breast skin surface 60 mm away, a paired transmission signal detection system is generated. The authors recruited 150 women between 30 and 50 years old to participate in this study. REIS measurements were performed on both breasts. Of these women 58 had been scheduled for a breast biopsy and 13 had been recalled for additional imaging procedures due to suspicious findings. The remaining 79 women had negative screening examinations. Eight REIS output signals at and around the resonance frequency were computed for each breast and the subtracted signals between the left and right breasts were used in a simple jackknifing method to select an optimal feature set to be inputted into a multi-feature based artificial neural network (ANN) that aims to predict whether a woman's breast had been determined as abnormal (warranting a biopsy) or not. The classification performance was evaluated using a leave-one-case-out method and receiver operating characteristics (ROC) analysis. The study shows that REIS examination is easy to perform, short in duration, and acceptable to all participants in terms of comfort level and there is no indication of sensation of an electrical current during the measurements. Six REIS difference features were selected as input signals to the ANN. The area under the ROC curve ($A_z$) was $0.707 \pm 0.033$ for classifying between biopsy cases and non-biopsy (including recalled and screening negative) and the performance ($A_z$) increased to $0.746 \pm 0.033$ after excluding recalled but negative cases. At 95% specificity, the sensitivity levels were approximately 20.5% and 30.4% in the two data sets tested. The results suggest that differences in REIS signals between two breasts measured in and around the tissue resonance frequency can be used to identify at least some of the women with suspicious abnormalities warranting biopsy with high specificity.  [DOI: 10.1118/1.2936221]

Key words: electrical impedance spectroscopy (EIS), impedance resonance, risk stratification, breast cancer detection, technology assessment

## I. INTRODUCTION

The risk of having or developing breast cancer at a young age is quite low but the number of person years lost due to deaths from this disease is disproportionably high because of longer life expectancy. As important perhaps, life loss at an early age, in particular premenopausal, is frequently associated with a significantly higher emotional and financial cost to the families involved as well as society as a whole. For some subgroups of young women the risk of developing breast cancer is significantly higher than average risk and these cancers are frequently more aggressive than the "average breast" cancer.[1] Because of the relatively low incidence and the fact that breasts of younger women tend to be denser due to a higher fraction of fibro-glandular tissue annual mammography examinations are generally not recommended for women younger than 40 years old and in some countries it is not recommended for women under the age of 50 years old.[2,3] It is well documented that the sensitivity and specificity of the mammography is relatively low in younger women.[4] A number of studies reported that for the younger women carrying one of two breast cancer susceptibility genes, BRCA1 and BRCA2, the sensitivity of conventional mammography only ranged from 16% to 40%.[5–7] The lower specificity of mammography also results in a higher recall for additional diagnostic procedures.[8,9]

To improve detection and diagnostic performance a number of imaging technologies have been investigated as alternative and/or adjunct approaches to mammography. In particular, the advent of full-field digital detectors with high resolution and large sensor size offer several opportunities for the development of advanced digital techniques that im-

prove conspicuity of breast lesions overlapped by fibroglandular tissue and enabling the enhancement of lesion contrast and in some cases enabling three-dimensional visualization of breast tissue structure. Imaging techniques including full-field digital mammography,[10] digital stereo-mammography,[11] digital breast tomosynthesis,[12] and cone beam breast computed tomography[13] have been attracting significant research and commercial development interests. The American Cancer Society has recently recommended periodic breast magnetic resonance imaging (MRI) examinations as an adjunct to mammography for screening women at high risk.[14] MRI has been shown to be sensitive for detecting breast cancers in several high-risk groups but to date the reported specificity of MRI is generally lower than that of mammography resulting in a higher recall rate.[14] In particular, MRI has low specificity for ductal carcinoma *in situ* and other types of invasive lobular cancers.[15] Other disadvantages in applying routine screening MRI to a substantial fraction of the population are cost, access, and the need for injection of contrast media. In reality the fraction of cancers in all known high-risk groups combined is relatively small as compared with the number of cancers in women with no known elevated risk factors.

Therefore, in the majority of younger women breast self-examination and clinical breast examination are the two most commonly employed non-imaging approaches employed in screening for breast cancer. These methods are not sensitive to the small, subtle, nonpalpable masses. Hence, the development of non-imaging, inexpensive, widely available, simple to use techniques to pre-screen younger women has been explored in recent years. The ultimate objective of these efforts is to stratify young women visiting their physicians (e.g., GP, GYN) into two groups. One group is "negative" or a group of women expected to have an average risk for having or developing breast diseases and the other one is "positive" or a group of women that should be considered for imaging based follow up (examinations). This strategy is a "rule in" strategy rather that a "rule our strategy" for women who would normally not participate in a periodic mammography or MRI screening program because they are too young and have no known risk factors or for other personal reasons. Namely, the use of such an approach may result in increasing overall compliance and as important, it would potentially result in a small fraction of younger women who are at significantly higher than average risk and would otherwise not be screened, to be recommended for and therefore undergo an imaging based follow-up. Hence, every additional cancer that would be found under this scenario will likely to be detected much earlier. The use of electrical impedance spectroscopy (EIS) is but one approach that has been investigated under this paradigm.[16] Differences in electrical impedance properties between benign and malignant breast tissue were identified as early as the 1920s.[17] A number of preliminary studies have shown that the EIS technology is inexpensive and easy to use. In particular, the EIS measurements perform reasonably well in dense breast tissue.[18–22] Currently, the only EIS device with U.S. Food and Drug Administration approval as an adjunct testing modality to mammography is the T-Scan 2000 (Mirabel Medical Systems, Austin, TX).[16] The algorithm used for this purpose is based on multiple logistic regression analysis of a wide range of frequency signals.[22] Despite the effort in applying EIS technology to detecting breast abnormalities, the use of current EIS systems is quite limited due primarily to the overall low sensitivity at high specificity. For example, 27% sensitivity at 94% specificity was reported when applying this technology to a group of women that included 36 positive and 476 negative cases.[22]

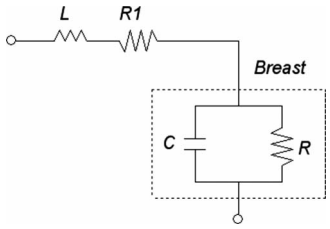


FIG. 1. A simplified schematic diagram of the REIS measurement circuit in which the breast is modeled as a resistor and a capacitor in parallel.

In this preliminary study, we developed and tested a rudimentary, unique, two probe (namely, one detection channel) prototype EIS system that produces continuous multifrequency pulse sweeps ranging from 100 to 4100 kHz. The signals being analyzed in this approach are specifically at and near the resonance frequency for the breast tissue being measured, hence, we term this approach resonance electrical impedance spectroscopy (REIS). Our main purpose and primary hypothesis in this very preliminary study were to validate that there is actual diagnostic information when using a rudimentary REIS system for this purpose and the ascertained information has a better than chance predictive value. The REIS device including methods of data acquisition and signal analysis as well as preliminary results, when applied to 150 women under an IRB approved protocol, are reported here.

## II. MATERIALS AND METHODS

### II.A. The prototype REIS device

The measurement of breast tissue response to the multifrequency electronic impedance sweeps are made by creating a circuit in which the breast is modeled as a resistor and a capacitor in parallel as shown in Fig. 1. The electrical circuitry has a wide multifrequency operating range of several megahertz. The inductor $L$ has a variable inductance and is varied until the resonance frequency of the entire circuit (including the measured breast tissue) falls within the operating frequency range of the system. Specifically, the resonance frequency is defined as the frequency at which the imaginary component of the impedance vanishes. In a collaborative effort between our imaging research group at the University of Pittsburgh and a commercial company (Kaiku Inc., Manchester, UK), we built a prototype REIS device (shown in Fig. 2). The REIS electronics control board includes all electronics that generate multifrequency sweeps of electronic

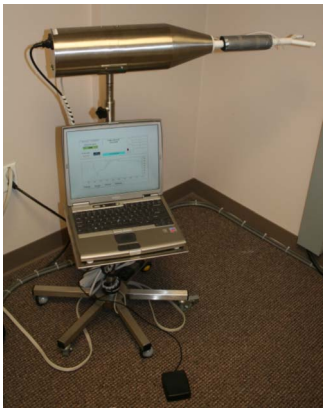

FIG. 2. Picture of the prototype REIS device with two probes as installed in our clinical breast imaging facility.

pulses ranging from 100 to 4100 kHz every 12 s and measures the received REIS output signals. The detected signals are recorded at 40 kHz increments. Thus, a total 101 REIS output signals are recorded during each sweep. The sensors (measurement probes) are two well shielded stainless steel electrodes. The two probes are mounted at the two ends of a Y-shape support device. Electrical impedance measurements are sensitive to the distance between probes, hence, in any system of this nature this distance has to be largely fixed. On one hand, one wishes to increase sensitivity to biological changes while covering as much tissue as possible between the probes, hence, the larger the distance between the probes the better the coverage that can be achieved. On the other hand, one wants to be able to measure all breast sizes in a relatively consistent manner. Therefore, after measuring a large number of breast sizes and in order to have one probe in contact with the nipple while the other touches the midline outer part of the breast, we semi-empirically selected a fixed 60 mm distance between the probes. The symmetry between the two probes allows for similar measurements to be acquired on both left and right breasts. For the purpose of this work, it is assumed that the measurements are insensitive to which of the probes is in contact with the nipple.

The maximum electric voltage and current applied to the two detection probes are 1.5 V and 30 mA, respectively. Hence, contact with the two probes at two points is similar to manually holding a 1.5 V battery. The measured REIS output signals are then digitized and transferred to a notebook computer attached to the system. In addition to processing and displaying the actual data, the computer also performs a number of control functions during the REIS examination, including patient information data entry, file opening, data recording, and generating a "start/stop" signals activated by a foot pedal (Fig. 2).

### II.B. REIS measurements and clinical database

The prototype REIS device has been installed in our clinical breast imaging facility. In this study, we focus on preliminary feasibility assessment for applying a REIS approach to measure the electrical impedance output signals and use a limited set of features extracted from these output signals to identify young women (<50 year old) who are suspicious during a traditional diagnostic work-up for having a breast abnormality that had been determined to warrant a biopsy. Under an IRB approved protocol, we recruited women who met the inclusion criteria in three categories. Women who consented to participate in this study underwent the REIS examination just prior to the scheduled clinical and/or imaging examinations. The REIS measurement results did not impact in any way the clinical management of participants and the investigators performing the data analyses were only given the REIS measurements data and an anonymously coded summary table with the group the participant belongs to and the outcome of the conventional clinical management of the participant. In the first group, we acquired REIS measurements on the left and right breasts of 79 women scheduled for a routine screening examination (without a prior recommendation for biopsy or being recalled). In the second group, we measured breast REIS on 13 women who had been determined during a prior examination (nine) or current examination (four) to have findings that warranted a recall (BIRADS 0). In the third group, we measured breast REIS on 58 women who had been scheduled for breast biopsy as a result of a previous diagnostic workup (BIRADS 4 or 5) within 4 weeks prior to the date of the biopsy. All participants were recruited sequentially by one qualified and trained health professional in the clinic and our inclusion criteria for women who had been recalled or those who had been scheduled for a biopsy did not include any restrictions regarding the type of abnormality in question or the location of the suspected abnormality within the breast. Using this REIS system, to date, we have acquired impedance measurements on 150 women who participated in this preliminary study. The average age of the participants and the standard deviation is $43.7 \pm 3.8$ years old (with a range of 30–50 years old).

During each REIS measurement procedure, the operator/technologist first uses the computer management program to open a new data file that includes participant information and is used to record the REIS output signal sweeps. The woman sits and uses one hand to hold ("lift") the breast being measured. The operator moves the REIS measuring device up or down to the appropriate height and then positions the woman to create good contact with the two probes, one in contact the nipple and the other with an arbitrary point on outer breast skin surface (centrally and approximately horizontally). The operator pushes (steps on) a foot pedal switch to initiate recording of the multifrequency REIS output signal sweeps. Since the electronic board continuously generates electrical pulse sweeps, motion of or change in contact with the probes can result in changes in the REIS output signal, the computer management program automatically monitors the changes between sequential sweeps of the REIS system every 12 s. The mean square difference between consecutive output signals of paired sequential sweeps at the same frequency level is computed as

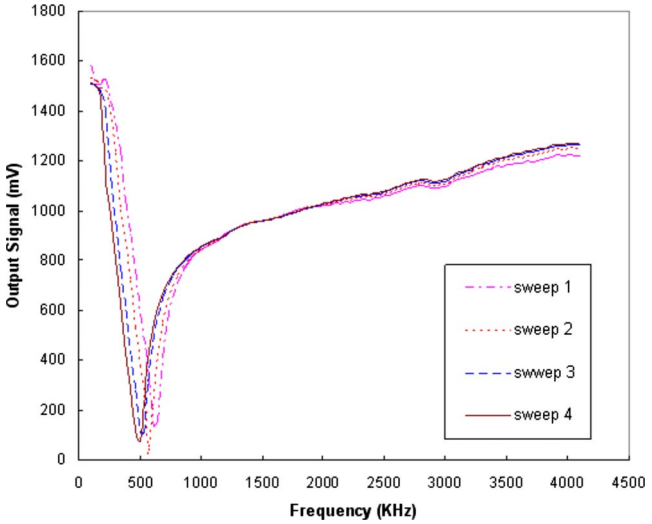


FIG. 3. An example of four sequential REIS multifrequency sweeps recorded on one breast. The sweeps shown in this example resulted in a "stable," hence, recorded sweep (No. 4).

$$\Delta S = \frac{1}{N}\sum_{i=1}^{N}[S_j(i) - S_{j-1}(i)]^2,$$

where $N=101$. If the mean signal difference between the current and the prior sweeps is larger than a default threshold (e.g., 5.0), the operating status displayed on the computer is "CHANGE" (in red color) indicating that the measured REIS sweep signals have not been stabilized. For example, as shown in Fig. 3, four sequential REIS sweeps are recorded. The computed differences in paired sequential REIS output measurements changes from 6.90 (between sweep 1 and 2), 8.56 (between sweep 2 and 3), to 4.87 (between sweep 3 and 4). Once the change is below the predetermined threshold, the operating status displayed on computer screen changes to "CONSISTENT" (in green color) and the operator pushes the foot pedal again to stop the recording. As shown in Fig. 3, the data file typically records multiple REIS output signal sweeps but only the last recorded REIS sweep in the data file is recognized as an acceptable measurement sweep (i.e., sweep No. 4 in Fig. 3). All prior REIS sweeps are considered "inconsistent" and discarded. The same procedure is applied to each breast. During the REIS data acquisition the woman is not required to hold her breath. Although possible body and breast movement is not directly or visually monitored, the quality (consistency) of the REIS measurement data itself is automatically assessed in real time by the REIS system. REIS measurement time for one breast ranged from 24 s (recording two REIS output signal sweeps) to 84 s (recording seven sweeps) before a CONSISTENT signal was displayed on the computer screen. The majority of measurements were completed within 48 s (i.e., four sweeps).

A "clinical status" or a "truth" file that includes the final diagnostic status of the 150 women included in this study was assembled and used in the data analyses. Among the 58 women who underwent biopsy, 44 depicted masses alone, ten depicted micro-calcification clusters alone, and four depicted both masses and micro-calcifications. The sizes (the largest axis length) of these masses as measured from the mammograms ranged from 0.2 to 5.0 cm with the mean value of 1.6 cm and standard deviation of 1.35 cm. The biopsy results show that four women were subsequently diagnosed with invasive breast cancer and the remaining 54 women were found to have a number of abnormalities including indraductal Papilloma, ductal epithelial hyperplasia, benign fibroadenomas, benign fibrocystic tissue, and other benign findings. Among the four verified cancer cases, two were associated with masses, one associated with a micro-calcification cluster alone, and one with both a mass and micro-calcifications. In the "recall" group of 13 women, 11 were ultimately be determined to have benign findings (i.e., benign cyst) and two did not return to our imaging facility for further examination to date. Thus, these two cases were excluded in our data analysis of this study.

TABLE I. Distribution of breast sizes of the 148 women whose data were analyzed in this study.

| Breast cup size | A | B | C | D | Total |
|---|---|---|---|---|---|
| Biopsy cases | 14 | 11 | 17 | 16 | 58 |
| Recall cases | 2 | 3 | 4 | 2 | 11 |
| Screening negative cases | 11 | 26 | 25 | 17 | 79 |

In summary, 148 REIS examinations are included in our data analyses. These cases are divided into two groups. The positive (biopsy) group includes 58 and the negative (nonbiopsy) group includes 90 cases. Among the 90 negative cases, 79 are screening verified negative cases (without recall) and 11 are negative that had been recalled for some suspected findings found initially on mammograms. Table I summarizes the distribution of breast sizes (as measured by bra size) of 148 women included in the analyzed data set and Fig. 4 shows the distribution of BIRADS density rating for the "biopsy" and "nonbiopsy" groups. As expected, based on the age distribution of the participants the majority of the

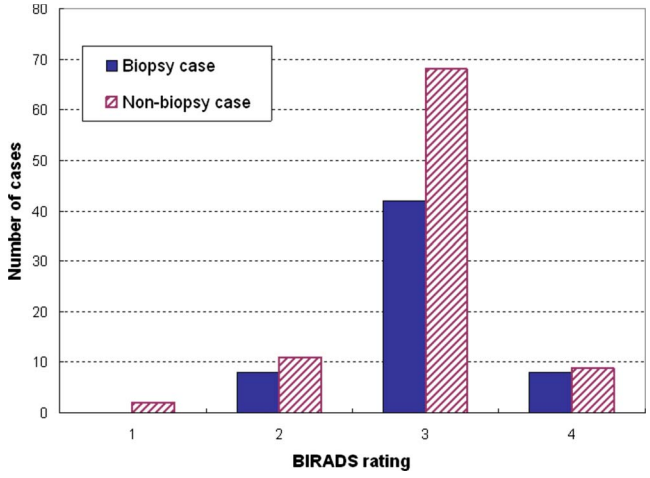


FIG. 4. Histogram of the breast tissue density BIRADS ratings for the 58 women scheduled to undergo biopsy and the 90 women who were not.

148 women were rated as having heterogeneously or very dense breast tissue (BIRADS category 3 or 4).

### II.C. Optimization and evaluation of an artificial neural network based classifier

The resonance frequency is defined as the frequency at which the output signal has a global minimum value in the REIS sweep (e.g., RF=500 kHz in sweep No. 4 of Fig. 3). At, below and above the resonance frequency, we computed following features: (1) the resonance frequency ($F_1$=RF), (2) the output signal value at the resonance frequency ($F_2 = V_{(RF)}$). For example, $V_{(RF)}$=80 mV in sweep No. 4 of Fig. 3. (3)-(8) the differences in output signals between that at the global minimum and signals at predetermined frequencies. Since REIS output data are recorded in an increment of 40 kHz, we extracted two output signals at frequencies smaller than resonance frequency (RF−80 kHz and RF−40 kHz) and at four output signals frequencies larger than the resonance frequency (from RF+40 kHz to RF+160 kHz). Thus, the six features are defined as the difference between output signal values at each of these frequencies and the output signal value at resonance frequency $V_{(RF)}$. They are $F_3 = V_{(RF-40)} - V_{(RF)}$, $F_4 = V_{(RF-80)} - V_{(RF)}$, $F_5 = V_{(RF+40)} - V_{(RF)}$, $F_6 = V_{(RF+80)} - V_{(RF)}$, $F_7 = V_{(RF+120)} - V_{(RF)}$, and $F_8 = V_{(RF+160)} - V_{(RF)}$).

In this study, we investigated the feasibility of using these simple REIS feature values to predict whether a woman may depict a suspicious breast abnormality resulting in a recommendation for biopsy (a case-based classification). A previous study reported a high correlation between left and right breast EIS measurements suggesting that breasts of the same women may have some impedance symmetry similar to the known symmetry of breast tissue patterns observed in mammograms.[23] Our own previous study also found that differences between REIS feature sets acquired from the two breasts (one abnormal and one negative) of the same biopsy cases were larger than those acquired from different cases.[24] Based on these findings, our underlying assumption in this study is that if a highly suspicious lesion (leading to a recommendation for a biopsy) is identified on one breast while the other breast is diagnosed as negative, asymmetry between the two breasts of the abnormal case should lead to differences in paired REIS features and therefore could be used in an attempt to discriminate between cases depicting a truly suspicious abnormality in one breast and those who do not.

To test this hypothesis, we subtracted the eight paired REIS feature values computed for the left and right breasts of each participant in our database ($\Delta F_i = |F_i^{\text{Left}} - F_i^{\text{Right}}|$, $i = 1,2,\ldots,8$) and recorded these eight REIS feature differences. We then used these differences ($\Delta F_i$, $i = 1,2,\ldots,8$) as input values to build an artificial neural network (ANN) based machine learning classifier designed to classify positive (biopsy) and negative (non-biopsy) cases. The ANN has a simple feed-forward three-layer topology. In the first layer each input neuron connects to one subtracted REIS feature value. For simplicity, in this preliminary study, the number of hidden neurons in the middle layer equals to half of the number of input neurons (e.g., eight input neurons and four hidden neurons). The output layer of the ANN has one neuron providing a classification score representing the likelihood of the case being abnormal (i.e., warranting a biopsy). The ANN is trained using the conventional backpropagation approach in which training iterations, training momentum, and learning rate were set at 500, 0.9, and 0.01, respectively.

Due to the limited size of our database we used the leave-one-case-out validation method to test the classification performance of the ANN.[25] Thus, each case is used 147 times for training and one time for testing. The 148 scores are used to fit a receiver operating characteristics (ROC)-type classification performance curve. The area under ROC curve ($A_z$) is used to represent a performance summary index. In addition, we used a feature jackknifing method to sequentially remove one of the eight features and used the remaining seven features to train and test eight different ANN sets each with seven input neurons and four hidden neurons. Thereafter, we trained and tested 28 ANN sets each with six input neurons and three hidden neurons by jackknifing (i.e., removing) two REIS difference features. Using this "exhaustive" permutation type jackknifing approach, we trained and tested total 37 ANNs. We then used the "progressive round-off" approach[26] to select five REIS difference features to build an "optimal" ANN set when using only five features. The highest performing ANN was selected to generate the optimal performance level for classification.

We conducted several additional experiments to evaluate the possible impact of case selection on the performance of our classification scheme. First, to test the possible effect of the 11 "recalled" cases included in the negative group, we repeated the analysis after excluding these recalled cases from the negative group and compared the results to the scenario when these are included in the negative group. Second, we reclassified the 11 recalled cases as positive and retested the performance of our scheme in classifying the cases in this new division into negative and positive groups. Third, we removed from the positive group the ten biopsy cases involving micro-calcification clusters alone and assessed if scheme performance changed, or not.

## III. RESULTS

Using the eight initial REIS difference features to train and test the ANN, the computed area under ROC curve ($A_z$) as a performance summary index. The results of this series of experiments were: (1) $A_z = 0.685 \pm 0.034$ when applying the ANN to classify all cases in our data set including 58 positive (biopsy) and 90 negative (nonbiopsy) cases; (2) After removing the 11 recalled cases from the negative group, $A_z$ value increased to $0.718 \pm 0.034$ (i.e., classifying between 58 biopsy and 79 screening negative cases); (3) reclassifying the 11 recalled cases as positive resulted in an $A_z$ of $0.701 \pm 0.033$; and, (4) removing the ten biopsy cases involving micro-calcification clusters alone resulted in an $A_z$ of $0.711 \pm 0.038$ when classifying between 48 biopsy cases depicting masses and 79 screening negative cases. The first

TABLE II. Summary of ANN performance ($A_z$ value) using seven of eight difference REIS features. (The standard deviations of the $A_z$ values are in the range between $\pm 0.033$ and $\pm 0.038$.)

| Removed feature | 1 | 2 | 3 | 4 | 5 | 6 | 7 | 8 |
|---|---|---|---|---|---|---|---|---|
| Including recalled cases | 0.672 | 0.684 | 0.632 | 0.687 | 0.683 | 0.664 | 0.682 | 0.626 |
| Excluding recalled cases | 0.734 | 0.715 | 0.704 | 0.711 | 0.732 | 0.702 | 0.692 | 0.653 |

three results [(1)–(3)] show a potential trend of increasing differences in paired REIS signals as measured on screening negative, recalled and biopsy cases. The last result (4) shows that the performance of our scheme was not substantially sensitive to whether breast abnormalities were depicted primarily as masses or micro-calcification clusters. These results are significantly ($p<0.001$) higher than chance ($A_z=0.5$).

Table II shows performance levels ($A_z$ values) when using seven of eight REIS difference features after removal of each of the input features. $A_z$ values ranged from 0.625 to 0.687 using all 148 REIS testing cases. After excluding the 11 recalled cases, $A_z$ values range from 0.653 to 0.734. The results show that removing either feature $\Delta F_1$ or $\Delta F_5$ result in higher performance level than that when using all eight features, but the improvements were not statistically significant ($p=0.059$ and $p=0.063$, respectively). On the other hand, removing either feature $\Delta F_7$ or $\Delta F_8$ significantly reduces the performance level of the scheme as compared with other ANN sets when using either seven or eight REIS difference features ($p<0.01$).

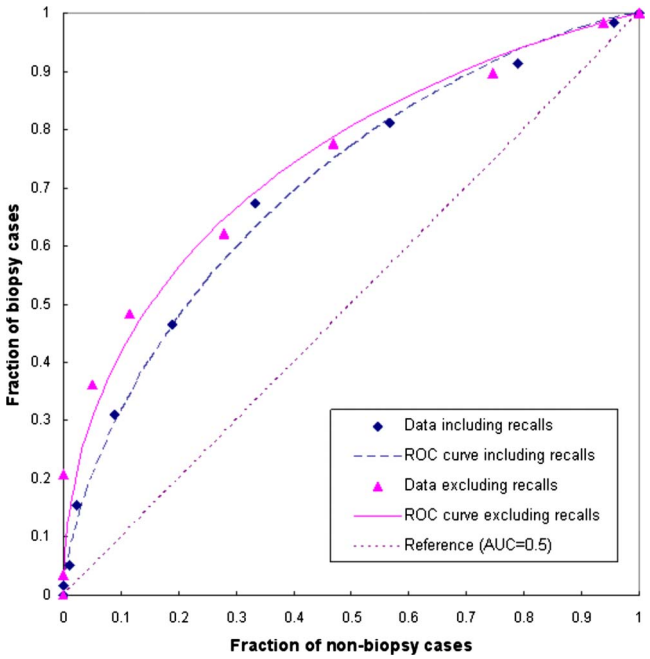


FIG. 5. Two ROC curves for classification of the 58 positive (biopsy) cases and the 90 negative (non-biopsy) cases with and after exclusion of the 11 recalled cases using the six REIS based features (difference in impedance measurements between left and right breasts) that resulted in the highest performance level ($0.707 \pm 0.031$, and $0.746 \pm 0.033$, respectively).

When jackknifing and using six REIS difference features to train and test ANNs, the average performance level of 28 ANNs was $A_z=0.656 \pm 0.045$ when testing all 148 cases. After excluding 11 recalled cases, the average performance level was $0.698 \pm 0.047$. The results show large variations in performance levels among these 28 ANNs. The highest performance level for all 148 cases ($A_z=0.707$) was generated when the ANN uses six features including $\Delta F_2$, $\Delta F_3$, $\Delta F_4$, $\Delta F_6$, $\Delta F_7$, and $\Delta F_8$ (or after removing $\Delta F_1$ and $\Delta F_5$); while excluding the 11 recalled cases the highest performance level ($A_z=0.746$) was achieved using six features namely, $\Delta F_1$, $\Delta F_3$, $\Delta F_4$, $\Delta F_6$, $\Delta F_7$, and $\Delta F_8$ (or after removing $\Delta F_2$ and $\Delta F_5$). The largest impact on the performance reduction was shown when both $\Delta F_7$ and $\Delta F_8$ were removed ($A_z=0.502$ for testing all 148 cases and $A_z=0.509$ when excluding the 11 recalled cases, respectively). Since a smaller impact was shown when either $\Delta F_1$ or $\Delta F_2$ or $\Delta F_5$ had been removed in the jackknifing experiment, our test result showed that using the "best" set of five REIS difference features ($\Delta F_3$, $\Delta F_4$, $\Delta F_6$, $\Delta F_7$, and $\Delta F_8$), the performance on all 148 cases was $A_z=0.696 \pm 0.033$ and on the 137 cases (excluding 11 "recalls") $A_z=0.742 \pm 0.034$.

Two sets of optimal (best) classification data and the corresponding ROC curves that represent the two highest performance levels when using six REIS difference features are shown in Fig. 5. These two performance curves show that at 95% specificity (5% "false-positive" detection rate) sensitivity levels are approximately 20.5% and 30.4% for the two data sets. We note that for the data set that excludes the 11 recalled cases, measured sensitivity levels in the range of interest (i.e., <0.1 false positive detection rate) are actually higher than those indicated by the fitted ROC curve (i.e., 36.2% sensitivity at 95% specificity). Tables III and IV show the actual (nonfitted) detection sensitivity levels of our scheme at different specificity levels when we include (Table III) and exclude (Table IV) the 11 recalled cases in the analysis. Table IV shows that under these conditions, 21 of 58 biopsy cases (36.2%) were detected at 95% specificity. Table V summarizes the characteristics of these 21 detected and actually positive cases. Among these, 16 depicted masses alone, three depicted microcalcification clusters alone, and two depicted both masses and microcalcifications, on mam-

TABLE III. Actual (non-fitted) detection sensitivity levels at different specificity levels when classifying biopsy and all nonbiopsy cases.

| Specificity (%) | 100 | 99 | 97 | 91 | 81 |
|---|---|---|---|---|---|
| Sensitivity (%) | 1.7 | 5.2 | 15.5 | 31.1 | 46.6 |

TABLE IV. Actual (nonfitted) detection sensitivity levels at different specificity levels when classifying biopsy and all screening negative cases after excluding the 11 recalled cases.

| Specificity (%) | 100 | 95 | 89 | 72 | 53 |
|---|---|---|---|---|---|
| Sensitivity (%) | 20.7 | 36.2 | 48.3 | 62.0 | 77.6 |

mograms. The sizes of the masses ranged from 0.5 to 4.5 cm. Large variations in breast size, mass size, and locations of the abnormalities in question within the breast are also shown.

## IV. DISCUSSION

The American Cancer Society advises that a regular screening mammographic examination be performed once a year on every woman 40 years old and continuing for as long as the woman is in good health.[2] As the number of women willing to be screened increases, so too does the demand placed on the health care system to deliver high quality examinations for such a large number of women while maintaining a reasonable cost associated with such a program. Of the women who undergo screening mammography each year, a significant fraction (6%–15%) will require additional imaging studies due to the suspicious findings.[9] Among them young women less than 50 years old are more likely to be recalled due to the inherent limitations of current mammography in diagnosing early disease in dense breast tissue. Although cancer prevalence rate among the young women is very low, invasive cancers developed in several higher risk subgroups of young women often have poor prognosis. Therefore, because of the low incidence of breast cancer in younger women, combined with the difficulties in diagnosing early disease in this group with conventional mammography, it may important to develop a low cost, easy to use prescreening tool with high specificity that could classify the younger women as having (or not) high risk for developing or having breast cancer that could potentially be detected at an earlier stage. This paradigm may be of particular interest for women who are younger than the recommended age for annual screening. Among the many possible alternative approaches, technology based on impedance measurements may prove to be a viable approach to this problem. It has been shown to detect breast abnormalities including cancer at an early stage.[18–22] In this preliminary and rudimentary study, we tested the feasibility of using a unique prototype REIS system that focuses primarily on comparing output signals between contralateral breasts near the resonance frequency of the evaluated breasts.

There are a number of differences between our REIS approach and previously developed EIS technologies. First, our REIS measurements are based on the detection of resonance frequency and assessments of REIS output signals (values) surrounding this resonance frequency. Second, our REIS system automatically indicates the recording of an "acceptable" or "stable" REIS measurement sweeps (signal output) by assessing in real time the magnitude of a change in the signal being measured (if any) between sequential sweeps. Therefore, our REIS measurement method provides a simple and potentially more robust approach to a successful completion of the examination. Our preliminary experience in this study indicates that the REIS examination is easy to perform, short in duration, and was acceptable to all 150 participants in terms of comfort level and no indication of sensation of an

TABLE V. Characteristics of the 21 "detected" biopsy cases at 95% specificity.

| Case | Breast (right/left) | Lesion type | Breast size (bra cup size) | Mass size (cm) | Location (o'clock) | Comments[a] |
|---|---|---|---|---|---|---|
| 1 | *R* | Mass | A | 0.6 | 9:00 | |
| 2 | *R* | Mass | C | 0.5 | 12:00 | |
| 3 | *L* | Mass | A | 0.7 | 9:30 | Periareolar |
| 4 | *R* | Mass | D | 1.9 | 12:00 | |
| 5 | *L* | Mass | D | 0.7 | 2:00 | 5 cm from the nipple |
| 6 | *R* | Mass | B | 1.5 | 9:00 | 4 cm superior to nipple |
| 7 | *R* | Calcifications | D | | 12:00 | Upper outer quadrant |
| 8 | *L* | Mass | B | 0.5 | 12:00 | Percutaneous |
| 9 | *L* | Mass | A | 1.2 | 5:00 | |
| 10 | *L* | Mass and calcifications | D | 1.0 | 3:00 | |
| 11 | *L* | Mass | D | 0.6 | 11:00 | Deep posterior |
| 12 | *L* | Calcifications | B | | 10:00 | Super-lateral to nipple |
| 13 | *R* | Calcifications | C | | 10:00 | |
| 14 | *R* | Mass | D | 2.4 | 12:00 | 10 cm from the nipple |
| 15 | *R* | Mass | A | 0.8 | 9:00 | Periareolar |
| 16 | *R* | Mass | A | 4.5 | 9:00 | |
| 17 | *R* | Mass | A | 1.9 | 9:00 | Far laterally |
| 18 | *L* | Mass | C | 1.3 | 6:30 | |
| 19 | *L* | Mass and calcifications | C | 0.8 | 5:00 | Lower inner quadrant |
| 20 | *R* | Mass | D | 0.7 | 12:00 | Superior retroareolar |
| 21 | *L* | Mass | B | 1.6 | 10:00 | Near chest wall |

[a]Comments (when specifically available) were recorded directly from the radiologists' reports.

electrical current during the measurements. To the best of our knowledge, no similar REIS system using this approach has been developed and tested for this purpose to date.

EIS measurement of breast tissue impedance characteristics is somewhat affected by the hormonal changes occurring during menopause (physiological age) and the overall breast tissue density of the patients.[16] Thus, based on the fact that electromagnetic symmetry between two negative breasts (left and right) is largely independent from patients' age and/or breast tissue density,[23] our approach uses REIS information from contralateral breasts during the feature analysis and classification. In this study we successfully demonstrated that for the purpose investigated here, the difference (or asymmetry) of REIS features surrounding the resonance frequency provide better information than independent information acquired solely from one breast.[24]

We emphasize that unlike mammography or other imaging technologies, EIS or REIS do not directly detect breast lesions nor does the system used here identify the location of the abnormality in question. It only detects changes (e.g., distortions) in electrical fields that may stem from biological changes (e.g., ductal epithelial changes). Similar to other studies[18,22] our results were not substantially sensitive to the type, size, or location of the lesions of interest. As long as the developing abnormality causes measurable distortions in the electrical field they have a nontrivial chance of being detected by the system. We note that while the distance between the probes may impact the results, the one we selected semi-empirically worked reasonably well in this prototype system, in that we were able to successfully and relatively easily obtain REIS measurements on women with widely varying breast sizes (as shown in Table I).

The two primary limitations of this study are the limited sample size and the rudimentary nature of the system as well as the computational approach used here. Although the initial results achieved using this simple prototype REIS system with a single detection channel (two probes) and the fixed probe distance are encouraging, it is clear that multichannel (probe) systems have to be developed and extensively tested on a large and diverse population to validate our initial findings and potentially improve performance. Further development of the REIS approach combined with optimization of feature selection and classification analyses are also needed before this technology can be seriously considered for routine use in the clinical practice as a low-cost, noninvasive, easy to use, prescreening, risk stratification tool.

## ACKNOWLEDGMENTS

This work is supported in part by a grant to the University of Pittsburgh from the National Cancer Institute, National Institute of Health (Grant No. 1R21CA127169). The authors also thank the Magee-Womens Research Institute and Foundation, Glimmer of Hope Fund, for supporting this effort.

[a]Electronic mail: zhengb@upmc.edu

[1]E. B. Claus, J. M. Schildkraut, W. D. Thompson, and N. J. Risch, "The genetic attributable risk of breast and ovarian cancer," Cancer **77**, 2318–2324 (1996).
[2]R. A. Smith, V. Cokkinides, and H. J. Eyre, "2003, American Cancer Society. American Cancer Society guidelines for the early detection of cancer," Ca-Cancer J. Clin. **53**, 27–43 (2003).
[3]R. A. Smith, "Breast cancer screening among women younger than age 50: A current assessment of the issues," Ca-Cancer J. Clin. **50**, 312–336 (2000).
[4]E. D. Pisano *et al.*, "Diagnostic performance of digital versus film mammography for breast cancer screening," N. Engl. J. Med. **353**, 1773–1783 (2005).
[5]M. Kriege *et al.*, "Efficacy of MRI and mammography for breast-cancer screening in women with a familial or genetic predisposition," N. Engl. J. Med. **351**, 427–437 (2004).
[6]M. O. Leach *et al.*, "Screening with magnetic resonance imaging and mammography of a UK population at high familiar risk of breast cancer: A prospective multicentre cohort study (MARIBS)," Lancet **365**, 1769–1778 (2005).
[7]E. Warner *et al.*, "Surveilance of BRCA1 and BRCA2 mutation carriers with magnetic resonance imaging, ultrasound, mammography, and clinical breast examination," J. Am. Med. Assoc. **292**, 1317–1325 (2004).
[8]D. B. Kopans, "The positive predictive value of mammography," AJR Am. J. Roentgenol. **158**, 521–526 (1991).
[9]J. J. Fenton *et al.*, "Reality check: Perceived versus actual performance of community mammographers," AJR Am. J. Roentgenol. **187**, 42–46 (2006).
[10]J. M. Lewin *et al.*, "Clinical comparison of full-field digital mammography and screen-film mammography for detection of breast cancer," AJR Am. J. Roentgenol. **179**, 671–677 (2002).
[11]D. J. Getty, P. M. Pickett, and C. J. D'Orsi, "Stereo-scopic digital mammography: Improving detection and diagnosis of breast cancer, Berlin, Germany," Int. Congr. Ser. **2001**, 506–511 (2001).
[12]L. T. Niklason *et al.*, "Digital tomosynthesis in breast imaging," Radiology **205**, 399–406 (1997).
[13]J. M. Boone, T. R. Nelson, K. K. Lindfors, and J. A. Seibert, "Dedicated breast CT: Radiation dose and image quality evaluation," Radiology **221**, 657–667 (2001).
[14]D. Saslow *et al.*, "American cancer society guidelines for breast screening with MRI as an adjunct to mammography," Ca-Cancer J. Clin. **57**, 75–89 (2007).
[15]A. S. Kumar *et al.*, "Biologic significance of false-positive magnetic resonance imaging enhancement in setting of ductal carcinoma *in situ*," Am. J. Surg. **192**, 520–524 (2006).
[16]A. Stojadinovic *et al.*, "Prospective study of electrical impedance scanning for identifying young women at risk for breast cancer," Breast Cancer Res. Treat. **97**, 179–189 (2006).
[17]H. Fricke and S. Morse, "The electric capacity of tumors of the breast," J. Cancer Res. **16**, 310–376 (1926).
[18]A. Malich *et al.*, "Electrical impedance scanning for classifying suspicious breast lesions: First results," Eur. Radiol. **10**, 1555–1561 (2000).
[19]T. E. Kerner *et al.*, "Electrical impedance spectroscopy of the breast: Clinical imaging results in 26 subjects," IEEE Trans. Med. Imaging **21**, 638–645 (2002).
[20]Y. A. Glickman *et al.*, "Novel EIS postprocessing algorithm for breast cancer diagnosis," IEEE Trans. Med. Imaging **21**, 710–712 (2002).
[21]J. H. Sumkin *et al.*, "Impedance measurements for early detection of breast cancer in younger women: A preliminary assessment," Proc. SPIE **5034**, 197–203 (2003).
[22]A. Stojadinovic *et al.*, "Electrical impedance scanning for the early detection of breast cancer in young women: Preliminary results of a multicenter prospective clinical trial," J. Clin. Oncol. **23**, 2703–2715 (2005).
[23]S. P. Poplack *et al.*, "Electromagnetic breast imaging: average tissue property values in women with negative clinical findings," Radiology **231**, 571–580 (2004).
[24]J. H. Sumkin *et al.*, "Assembling a prototype resonance electrical impedance spectroscopy system for breast tissue signal detection: Preliminary assessment," Proc. SPIE **6917**, 16-1-8 (2008).
[25]Q. Li and K. Doi, "Reduction of bias and variance for evaluation of computer-aided diagnostic schemes," Med. Phys. **33**, 868–875 (2006).
[26]K. McAloon and C. Tretkoff, *Optimization and Computational Logic* (Wiley, New York, 1996), pp. 50–53.